2020-08

Flow and magnetic structures in a kinematic ABC-dynamo

Zhang, T

10.1007/s11433-019-1568-x
Science China Physics, Mechanics & Astronomy
Springer Science and Business Media LLC

SCIENCE CHINA
Physics, Mechanics & Astronomy

• Letter to the Editor •

? ? Vol. ? No. ?: ??
doi: ??

1

Flow and magnetic structures in a kinematic ABC-dynamo

Tao Zhang[1], Zhiliang Lin[1,2*], Chenyang Huang[1], and Alistair G. L. Borthwick[3]

[1] *State Key Laboratory of Ocean Engineering, School of Naval Architecture, Ocean and Civil Engineering, Shanghai Jiao Tong University, Shanghai 200240, China*
[2] *Collaborative Innovation Center for Advanced Ship and Deep-Sea Exploration, Shanghai 200240, China*
[3] *School of Engineering, The University of Edinburgh, Edinburgh EH9 3JL, United Kingdom*

Received Dec., 2019; accepted ?; published online ?

Dynamo theory describes the magnetic field induced by the rotating, convecting and electrically conducting fluid in a celestial body. The classical ABC-flow model represents fast dynamo action, required to sustain such a magnetic field. In this paper, Lagrangian coherent structures (LCSs) in ABC-flow are detected through Finite-time Lyapunov exponents (FTLE). The flow skeleton is identified by extracting intersections between repelling and attracting LCSs. For the case $A = B = C = 1$, the skeleton structures are made up from lines connecting two different types of stagnation points in the ABC-flow. The corresponding kinematic ABC-dynamo problem is solved using a spectral method, and the distribution of cigar-like magnetic structures visualized. Inherent links are found to exist between LCSs in the ABC-flow and induced magnetic structures, which provide insight into the mechanism behind the ABC-dynamo.

kinematic dynamo theory, ABC-flow, lagrangian coherent structure

PACS number(s): 91.25.Cw, 91.25.Mf, 47.27.De

Citation: Tao Zhang, Zhiliang Lin, Chenyang Huang, and Alistair G. L. Borthwick, Flow and magnetic structures in a kinematic ABC-dynamo, Sci. China-Phys. Mech. Astron. **?**, ?? (?), doi: ??

1 Introduction

In 1965, Arnold [1, 2] discovered a class of analytical solutions of the Euler equations whose flow exhibited "fast dynamo" action. This type of flow was later named Arnold-Beltrami-Childress (ABC) flow, and may be expressed as:

$$\begin{cases} \dot{x} &= A\sin z + C\cos y \\ \dot{y} &= B\sin x + A\cos z \\ \dot{z} &= C\sin y + B\cos x \end{cases} \tag{1}$$

where x, y and z are tracer locations in cartesian space, A, B and C are three prescribed parameters that control the dynamo action of the flow. In 1986, Dombre et al. [3] identified a relationship between the three parameters and the positions of different categories of flow stagnation points. In the same year, Galloway et al. [4] investigated the properties of a fast dynamo flow by varying the magnetic Reynolds number with prescribed values of the parameters A, B, and C, and discovered the presence of cigar-like structures in the magnetic field. In 2003, Archontis et al. [5, 6] separately combined the magnetic field with laminar and turbulent flow fields, and found that the difference in growth rate is due to discrepancies in the recycling of the weakest part of the magnetic field. They also analyzed the properties of the resulting magnetic structures. In 2013, Bouya et al. [7] examined the dynamo properties of a flow at high magnetic Reynolds number and analyzed discontinuous jumps in the imaginary part of the dominant eigenvalue of the eigenmode with the largest growth rate. Meanwhile, Alexakis et al. [8] searched the entire family of ABC-flows for dynamo action. Alexakis et al. found the maximum growth rates at different magnetic Reynolds numbers, and observed that cases with maximum growth rate corresponded to the maximum finite time

[1] *Corresponding author (email: linzhiliang@sjtu.edu.cn.)

Lyapunov exponent (FTLE). In additional, with the help of FTLE, Zienicke et al. [9] studied the reaction of the magnetic field on the ABC-flow field in different phases of the dynamo.

Based on the FTLE, Haller's team [10-13] proposed a method for efficiently detecting Lagrangian coherent structures (LCSs), which has since proved useful in studies of nonlinear dynamic systems (such as chaotic flow, and turbulence) [11]. In 2013, Rempel et al. [14] applied both the Eulerian(Q-criterion) and Lagrangian(M-function) tools to reveal the flow and magnetic structures in a nonlinear dynamo and demonstrated that Lagrangian analysis can better locate the boundaries of vortices and provide important information about the mixing properties of the flow. Inspired by the discussions of the correlation between the flow and magnetic fields in dynamo problems by Archontis et al. [5] and Galloway [15], this letter applies the FTLE to identify newly defined skeleton structures in a full symmetry ABC-flow ($A = B = C = 1$), and then explores the relation between flow structures in the induced kinematic dynamo with the associated magnetic structures.

2 Numerical results

The computational domain in this work is set as a cube of side length 2π. In the present calculation of the FTLE field, the computations commence with a $200 \times 200 \times 200$ uniform grid of tracer particles. A fourth-order Runge-Kutta method is used for time integration, and the time interval T is set as 5. The parameter setting could refer to Haller's work [12]. Figures 1 (a) and (b) show the iso-surfaces which correspond to high FTLE values of the forward and backward time calculations. These regions consist of piecewise smooth surfaces that respectively represent repelling and attracting surfaces in the flow field. By utilizing the addition Lyapunov exponent E_T (see Supporting Information) and taking iso-surfaces of E_T with $E_T = 0.9E_{Tmax}$ (where E_{Tmax} represents the maximum value of E_T in the flow field), the intersecting lines are extracted, as shown in Figure 1 (c). These intersections between repelling and attracting surfaces therefore define the skeleton structures of the 3-D flow field.

The ABC-flow in this letter contains a number of internal symmetries. As can be seen in Figure 1 (c), the skeleton structures exhibit high symmetry. Each skeleton consists of line segments, whose endpoints point to certain fixed points which coincide exactly with flow stagnation points. Dombre et al. [3] classified stagnation points into two types according to the eigenvalues of the velocity gradient matrix $\nabla \mathbf{u}_s$, with type α stagnation points having two negative eigenvalues and type β having two positive eigenvalues. Herein, we use the same classification of stagnation points, but different criteria, noting that motions of fluid particles on the skeleton structures display certain differences. In Figure 1 (c), the different types of stagnation points in the adjacent areas are marked S and G. Fluid particles on the skeleton structures near an α-type stagnation point (red) are repulsed and stretch apart along the skeleton structures. Such stagnation points are denoted as S_i ($i = 1, 2, 3, 4$) (corresponding to α-type stagnation points). Conversely, fluid particles on skeleton structures are attracted to the β-type stagnation points (blue). Such stagnation points are denoted G_i (corresponding to β-type stagnation points). The properties of particles on the skeleton structures are also supplied in Supporting Information.

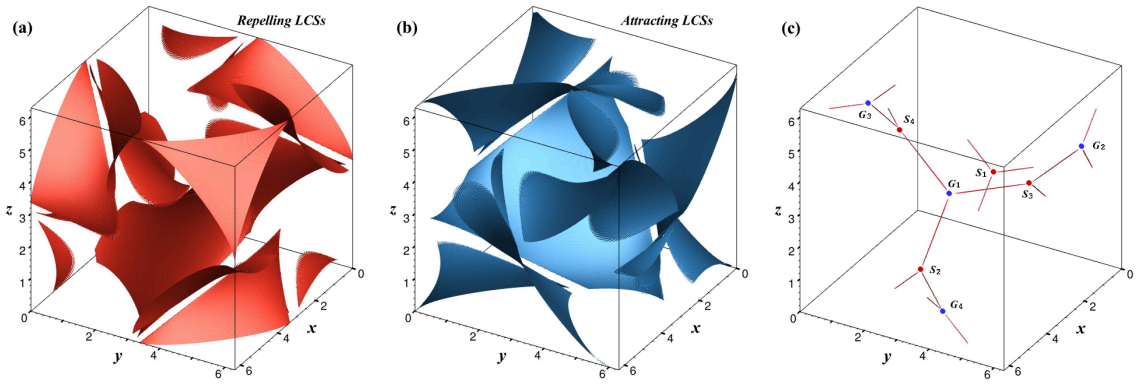

Figure 1 Lagrangian coherent structures and their skeletons in an ABC-flow with $A = B = C = 1$ and $T = 5$: (a) repelling LCSs; (b) attracting LCSs; and (c) skeletons defined by the iso-surfaces with $E_T = 0.9E_{Tmax}$. The marked points S_i and G_i ($i = 1, 2, 3, 4$) correspond to α-type and β-type stagnation points [3].

Considering the magnetic field induced by the symmetric ABC flow, Figure 2 displays the changes occurring to the magnetic structures during turnover of the magnetic field. The selection of the magnetic Reynolds number (R_m) as 120 and the numerical simulation of the kinematic dynamo are given in Supporting Information. Iso-surfaces where the magnetic field has high strength ($ME = 0.3ME_{max}$) are used to reveal the magnetic structures, which appear as cigar-like shapes in the flow domain. Due to the periodicity of the space, four cigar-like structures can be seen (marked M_1, M_2, M_3 and M_4). Three of the cigar-like structures respectively pass through the front and back, left and right, and upper and lower surfaces of the cubic body. The fourth cigar-like structure exists along a diagonal of the cube. These structures contain most of the magnetic energy in the field and their respective evolutions are able to explain the change in

total magnetic energy. At $t = 155$, the M_1 structure starts to disappear due to turnover of its inner magnetic field. Thus the total energy growth rate is decreasing (see Figure S1 in Supporting Information). At $t = 177.5$, the total energy experiences a local cusp-like minimum caused by turnover of the other three structures. As can be seen in Figure 2 (b), the only structure in the field is M_1. At this instant in time, the magnetic field inside M_1 has already reversed. Afterwards, the other three structures reverse and reappear. In Figure 2 (c), at $t = 200$, we again see the four cigar-like structures, which each contain almost the same energy.

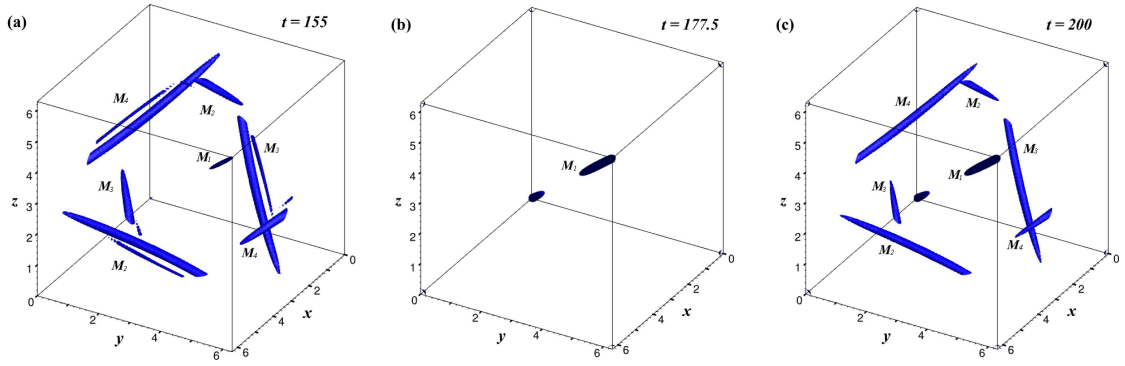

Figure 2 Magnetic structures represented by the isosurface of magnetic energy $ME = 0.3ME_{max}$ for $Rm = 120$ and $A = B = C = 1$ at (a) $t = 155$, (b) $t = 177.5$, and (c) $t = 200$ (The three instants correspond to blue dots a, b and c in Figure S1 of Supporting Information).

During this turnover process (from $t = 155$ to $t = 200$), the behaviour of structure M_1 is different from that of the others. We call M_1 the principal magnetic structure (MS), and the other three auxiliary MSs. In fact, the locations of the four cigar-like structures shown in Figure 2 (c) can all be candidate locations for the principal MS when choosing the appropriate seed field (see Supporting Information).

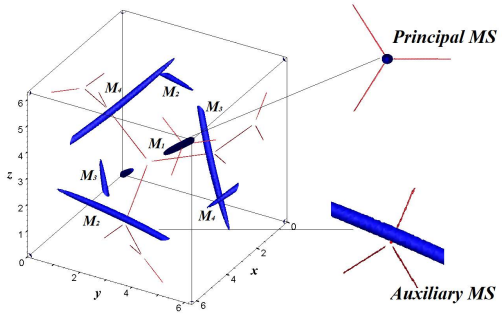

Figure 3 Strong link between LCSs and magnetic structures at $t = 200$. The red line structures are LCSs (iso-surface with $E_T = 0.9E_{Tmax}$) whereas the blue cigar-like structures are magnetic structures (iso-surface with $ME = 0.3ME_{max}$). The axis of the principal magnetic structure along the diagonal of the cube exactly passes through S_2 and points to G_2. The auxiliary magnetic structure is located near S_4. The blue columnar structure is a little curved and does not quite pass through S_4.

3 Relation between the magnetic and flow structures

Given that the magnetic field is induced by the flow field, it is quite natural to expect that the magnetic field structures should be controlled by the flow. (It should be noted that Archontis et al. [5, 6] have already come to similar conclusions from an Eulerian viewpoint.) Therefore, the relationship between structures of the flow and magnetic fields warrants further consideration.

In order to study all of the four complete structures, we now focus on the instant when $t = 200$. Figure 3 superimposes both the magnetic and flow structures at the same time, from which it can be seen that there is a certain relationship between both sets of structures. First, the principal MS (M_1) passes through S_1 (α-type stagnation point as shown in Figure 1 (c)). The other three auxiliary MSs (M_2, M_3, M_4) almost pass through the other three α-type stagnation points (S_2, S_3, S_4), respectively. In addition, the cigar like structures all seem to be intermittent in the vicinity of the β-type stagnation points, which was also reported in the previous work by Galanti et al. [16]. Geometrically, the principal MS is perpendicular to the plane formed by the three lines in the skeleton structures of the flow field, i.e., G_1S_2, G_1S_3 and G_1S_4. A brief proof is provided in Supporting Information.

The top right corner of Figure 3 coincides with the principal magnetic structure viewed from a diagonal perspective. The principal magnetic structure is columnar, coinciding with the diagonal and completely passing through S_1. Turning to the auxiliary MSs and taking the structure near S_4 as an example, the bottom right corner of Figure 3 shows details of the magnetic structure M_2. Unlike the principal axis, the remaining three structures (M_2, M_3, M_4) are curved slightly, and their axes do not pass through the corresponding stagnation points (a certain offset exists for each auxiliary magnetic structure). The possible reason for these offsets is that the principal MS is more advanced in the turnover process, which means that it acts as a precursor and attract the other MSs.

The binding of magnetic structures to the flow skeleton can be illustrated by expansion of the cube due to its 2π-periodic

property in the x, y and z directions. For example, the principal MS (M_1) after space expansion is shown in Figure 4. M_1 is bound by the net-like skeleton of the fluid flow. Each M_1 is associated with three layers of flow skeleton structures, all of which are parallel to each other and perpendicular to the centre axis of M_1. The middle layer is centred at S_1, which is also the core of M_1, and equally surrounded by three β-type stagnation points (G_2, G_3 and G_4). The outer two layers are planes, each of which is expanded by three skeleton lines centred at G_1 that are directed radially through the α-type stagnation points (S_2, S_3 and S_4). The three auxiliary MSs (M_2, M_3 and M_4) have the same binding property, but due to their secondary attraction to the principal MS (M_1), they undergo some bending and so cannot pass exactly through their corresponding α-type stagnation points.

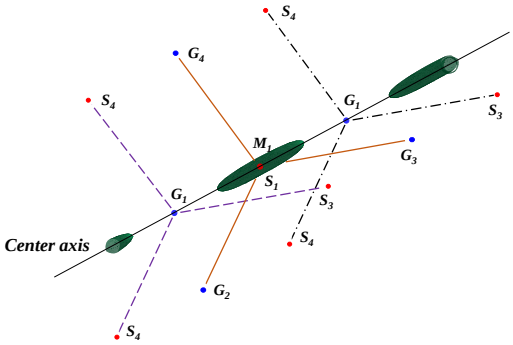

Figure 4 Part of the expanding flow and magnetic structures (principal MS). The flow skeleton structures act as a net and constrain the magnetic structures. Three layers are considered as a whole (the outer layers are dotted). The center axis of M_1 is perpendicular to the layers and G_1 and S_1 are located along this axis.

To explore the energy concentration of the magnetic field and the distribution of the cigar-like structures, it is useful to examine the velocity field of the fluid flow from an Eulerian viewpoint. Figure 5 (a) shows the iso-surface of the largest velocity in the flow with the magnetic cigar-like structures superimposed. It can be seen that, within the cube $[0, 2\pi]^3$, there exist 8 small zones of highest flow velocity that are distributed at the two ends of each cigar-like structure which are relatively small and sharp. But the central part appears thicker. Obviously, the flow velocity distribution from an Eulerian viewpoint is not sufficient to explain the formation of the magnetic structures.

Figure 5 (b) shows the repelling Lagrangian coherent structures in the ABC-flow for $T = 1$, which comprise small disc-shaped iso-surfaces. The repelling structures are located at α-type stagnation points (S_i) where the magnetic field has strongest intensity. The reason could be that the repelling LCSs represent the place with the most stretching ability which is the key for the dynamo effect.The disc-shaped repelling LCS is at the center of and substantially perpendicular to the cigar-like magnetic structure. Figure 5 (c) shows the attracting Lagrangian coherent structures, which are similar to the flux sheets mentioned by [5], obtained by calculation of the FTLE over a short time interval $T = 1$. Attracting LCSs are located at β-type stagnation points (G_i) and also comprise small disc-shaped iso-surfaces. Thus, the cigar-like magnetic structures are constrained into the space between two adjacent attracting LCSs, and so the β-type stagnation points behave as barriers that cut the magnetic field columns into the observed cigar-like structures.

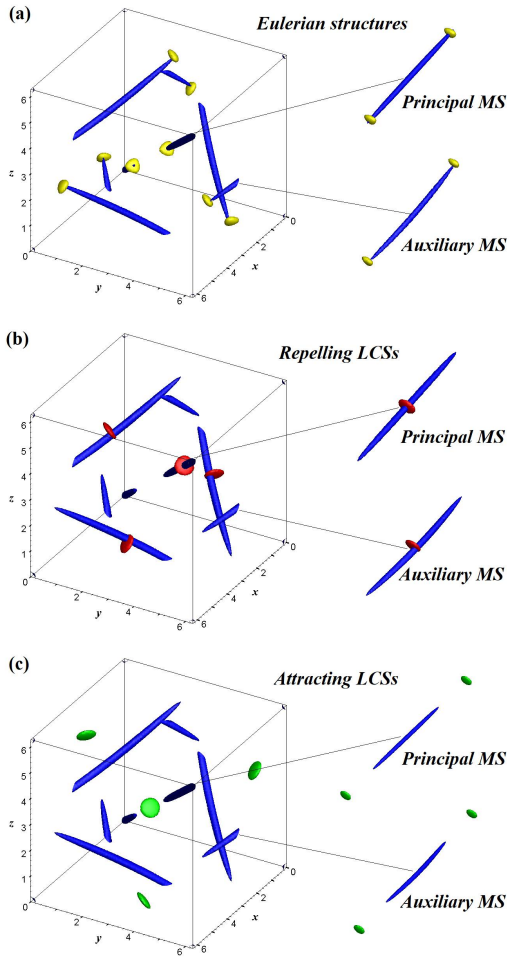

Figure 5 (a) Eulerian structures with maximum velocity in the ABC-flow field, which are invariably located at both ends of the magnetic cigar-like structures; (b) Repelling Lagrangian coherent structures in the ABC-flow for $T = 1$, which are all located at α-type stagnation points where the magnetic intensities are the strongest; (c) Attracting Lagrangian coherent structures in the ABC-flow for $T = 1$, which are all located at β-type stagnation points where the magnetic intensities are zero. (Topological extensions of the principal and auxiliary magnetic structures are included on the right side of each cube.)

4 Conclusions

To sum up, a fully new flow skeleton is defined as intersections of repelling and attracting LCSs, which can clearly explore the binding of magnetic structures with the ABC-flow. Besides, the results in this letter demonstrate that Lagrangian coherent structures (both repelling and attracting LCSs) are

more helpful in exploring the distribution and shape of magnetic structures in ABC-flows. Knowledge of the correlation between flow and magnetic structures should enable better understanding of the mechanism of dynamo effect but more works need to be done. In future work, we intend to consider: magnetic fields induced by other types of ABC-flow (with 4 or 0 stagnation points); the effect of flow structures on evolution of the magnetic field, in particular the magnetic field reversal phenomenon; and the correlation between flow and magnetic structures in dynamical dynamo problems.

This work was supported by the National Natural Science Foundation of China (Grant No. 51979162).

Supporting Information

The supporting information is available online at phys.scichina.com and link.springer.com. The supporting materials are published as submitted, without typesetting or editing. The responsibility for scientific accuracy and content remains entirely with the authors.

1 V. I. Arnold, *Vladimir I. Arnold-Collected Works* (Springer, 1965) p. 15–18.
2 V. I. Arnold, Y. B. Zel'dovich, A. A. Ruzmalkin, and D. D. Sokolov, J. Exp. Theor. Phys. **81**, 2052–2058 (1981).
3 T. Dombre, U. Frisch, J. M. Greene, M. Hénon, A. Mehr, and A. M. Soward, J. Fluid Mech. **167**, 353–391 (1986).
4 D. Galloway, and U. Frisch, Geophys. Astrophys. Fluid Dyn. **36**, 53–83 (1986).
5 V. Archontis, S. B. F. Dorch, and Å. Nordlund, Astron. Astrophys. **397**, 393-399 (2003).
6 V. Archontis, S. B. F. Dorch, and Å. Nordlund, Astron. Astrophys. **410**, 759–766 (2003).
7 I. Bouya, and E. Dormy, Phys. Fluids. **25**, 037103 (2013).
8 A. Alexakis, Phys. Rev. E. **84**, 026321 (2011).
9 E. Zienicke, H. Politano, and A. Pouquet, Phys. Rev. Lett. **81**, 4640-4643 (1998).
10 G. Haller, and G. C. Yuan, Physica D. **147**, 352–370 (2000).
11 G. Haller, Annu. Rev. Fluid Mech. **47**, 137–162 (2015).
12 G. Haller, Physica D. **149**, 248–277 (2001).
13 H. Teramoto, G. Haller, and T. Komatsuzaki, Chaos. **23**, 043107 (2013).
14 E. L. Rempel, A. C. L. Chian, A. Brandenburg, and P. R. Muñoz, J. Fluid Mech. **729**, 309-329 (2013).
15 D. Galloway, Geophys. Astrophys. Fluid Dyn. **106**, 450–467 (2012).
16 B. Galanti, P. L. Sulem, and A. Pouquet, Geophys. Astrophys. Fluid Dyn. **66**, 183-208 (1992).